Structure and Dynamics of Low-Density and High-Density Liquid Water at High Pressure

ARTICLE *in* JOURNAL OF PHYSICAL CHEMISTRY LETTERS · DECEMBER 2013

Impact Factor: 7.46 · DOI: 10.1021/jz402302z

THE JOURNAL OF PHYSICAL CHEMISTRY Letters

Letter

pubs.acs.org/JPCL

Structure and Dynamics of Low-Density and High-Density Liquid Water at High Pressure

Samuele Fanetti,[†] Andrea Lapini,[†,‡] Marco Pagliai,[‡] Margherita Citroni,[†,‡] Mariangela Di Donato,[†,‡] Sandro Scandolo,[§] Roberto Righini,[†,‡] and Roberto Bini*[,†,‡]

[†]LENS, European Laboratory for Non-linear Spectroscopy, Via N. Carrara 1, I-50019 Sesto Fiorentino, Firenze, Italy

[‡]Dipartimento di Chimica "Ugo Schiff" dell'Università degli Studi di Firenze, Via della Lastruccia 3, I-50019 Sesto Fiorentino, Firenze, Italy

[§]The Abdus Salam International Centre for Theoretical Physics (ICTP), Strada Costiera 11, I-34151 Trieste, Italy

ABSTRACT: Liquid water has a primary role in ruling life on Earth in a wide temperature and pressure range as well as a plethora of chemical, physical, geological, and environmental processes. Nevertheless, a full understanding of its dynamical and structural properties is still lacking. Water molecules are associated through hydrogen bonds, with the resulting extended network characterized by a local tetrahedral arrangement. Two different local structures of the liquid, called low-density (LDW) and high-density (HDW) water, have been identified to potentially affect many different chemical, biological, and physical processes. By combining diamond anvil cell technology, ultrafast pump−probe infrared spectroscopy, and classical molecular dynamics simulations, we show that the liquid structure and orientational dynamics are intimately connected, identifying the $P-T$ range of the LDW and HDW regimes. The latter are defined in terms of the speeding up of the orientational dynamics, caused by the increasing probability of breaking and reforming the hydrogen bonds.

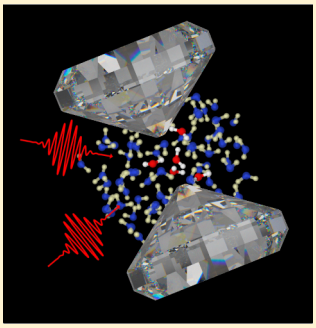

SECTION: Liquids; Chemical and Dynamical Processes in Solution

Water exhibits a remarkably rich phase diagram, and even within the liquid phase its properties change as a function of pressure and temperature in unconventional ways.[1] The structure of liquid water is characterized by the molecular self-association through hydrogen bonds, believed to be crucial in explaining most of its anomalous properties.[2] On the molecular scale, this structure changes dynamically as H bonds are continuously destroyed and reformed to accomplish rotational motions of individual molecules.[3] In the $P-T$ range of thermodynamic stability of the liquid phase, two different local structures (LDW and HDW) have been revealed by neutron diffraction studies[4,5] with a macroscopic density difference of ∼30%.[4] In both forms, the first coordination shell remains tetrahedral, but a shortening of the mean distance of the second coordination shell, which collapses onto the first one, is observed approaching the HDW structure. Small-angle X-ray scattering showed the coexistence under ambient conditions of domains (mean size ∼1 nm) of the two forms in dynamic equilibrium.[6] Any change in T or P affects the H-bond interactions and shifts the equilibrium between the two forms in a continuous way. An analogous picture results from classical molecular dynamics simulations, with a first shell of H-bonded molecules almost unaffected by pressure, whereas the second-shell molecules approach the interstitial sites of the first tetrahedral shell as the pressure increases to give rise to the HDW structure.[7] Among the theoretical approaches developed to provide structural models capable of explaining the static and dynamical properties of water, the second critical point hypothesis,[8] the singularity-free scenario,[9,10] and the critical point-free scenario[11] suggest that two water forms can exist in the supercooled regime as liquid counterpart of low-density and high-density amorphous ice.[12,13] Besides the aforementioned neutron scattering studies, inelastic X-ray scattering,[14,15] Brillouin,[16] and Raman[17] experiments have been performed at high pressure to identify signatures of the two structures and possibly locate the transformation without reaching conclusive results. From this overview pressure turns out to be a powerful method to change the relative amount of the two species whose coexistence should not be seen as the equilibrium between two macroscopically distinct phases but rather as a dynamical phenomenon as they reciprocally interconvert exploring innumerable intermediate configurations. To address the behavior of water when pressure and temperature are tuned in the thermodynamic stability range of the liquid phase, we have investigated samples compressed in a sapphire anvil cell by ultrafast infrared pump−probe spectroscopy, a technique able to provide detailed information on the orientational motion of water molecules[18] and on the ultrafast dynamics of the hydrogen-bond network,[19,20] which rules the local structure build-up and transformation. Pump−probe ultrafast spectroscopy has never been used in conjunction with ultrahigh pressure devices to access the gigapascal (GPa) range. This is indeed a challenging experiment due to the small sample

Received: October 24, 2013
Accepted: December 19, 2013
Published: December 19, 2013

dimensions and to its reduced thickness (50 μm) with respect to the diamond or sapphire anvils (2 to 3 mm each) in which it is contained. Finally, through classical molecular dynamics calculations, we were able to correlate structural and dynamical properties providing information about the nature and the existence range of LDW and HDW.

We performed femtosecond mid-infrared pump−probe spectroscopy on mixtures of D_2O in H_2O, compressed in a membrane anvil cell equipped with sapphires, measuring the anisotropy decay time constant (τ_R) and the vibrational lifetime (τ_v) of the OD stretching vibration at two different temperatures (298.0 and 363.1 K) from ambient pressure up to 1 GPa. We used the OD stretching mode as a probe of the water dynamics because of its spectral isolation and of the vanishing absorption of sapphire in this spectral region (~2500 cm^{-1}). In addition, the OD vibration is a suitable probe of the water behavior[21] because its dynamics depends on the strength of the H bond and on how the local structure of the surrounding water molecules is modified by pressure and temperature. Furthermore, resonant energy transfer between neighbor OD oscillators is negligible at the low D_2O concentration adopted,[22] so that the anisotropy decay reflects only the molecular reorientation and is a direct measurement of the external motion of water molecules. These data are completed by linewidth FTIR measurements of the OD stretching band at 273.7, 298.0, and 363.1 K as a function of pressure.

In the ultrafast pump−probe experiment, a broadband IR pump pulse excites the OD vibration, and the induced transient absorption is monitored by a second IR pulse probing the excitation at different time delays. The ratio between the probe intensity with and without the pump pulse, normalized to the reference beam, gives the differential absorption spectrum, which is recorded as a function of the pump−probe time delay. The room-temperature transient absorption spectra measured at 0.18 GPa are reported in Figure 1. The rotation free $\Delta\alpha_{iso}(t)$ and anisotropic $R(t)$ signals are obtained by recording the differential spectra with parallel and perpendicular polarization between pump and probe and calculated according the following relations:

$$\Delta\alpha_{iso}(t) = \frac{\Delta\alpha_{\parallel}(t) + 2\Delta\alpha_{\perp}(t)}{3} \quad (1)$$

$$R(t) = \frac{\Delta\alpha_{\parallel}(t) - \Delta\alpha_{\perp}(t)}{3\Delta\alpha_{iso}(t)} \quad (2)$$

To calculate the correct anisotropy decay and vibrational relaxation times, we corrected the data for the time-dependent thermal signal as reported in refs 23−26. The vibrational energy relaxation (b) and the depolarization rate of excitation $R(t)$ (c) at some selected pressures are reported in Figure 1. Relevant changes in $R(t)$ are observed at 298.0 K between ambient pressure and 0.2 GPa, but further compression up to 0.9 GPa has a small effect on the anisotropy decay.

The vibrational energy relaxation and the corrected $R(t)$ were then fitted by a single exponential function to obtain the time constants τ_v and τ_R, which are reported as a function of density for two different temperatures in Figure 2. Here the pressure and temperature effects are extremely evident. At 363.1 K, no relevant slope changes are observed for both τ_v and τ_R, whereas at 298.0 K a clear slope change is observed for both parameters around 1070 kg/m^3 (~0.2 GPa). Density values were computed by the equation of state of fluid water.[27]

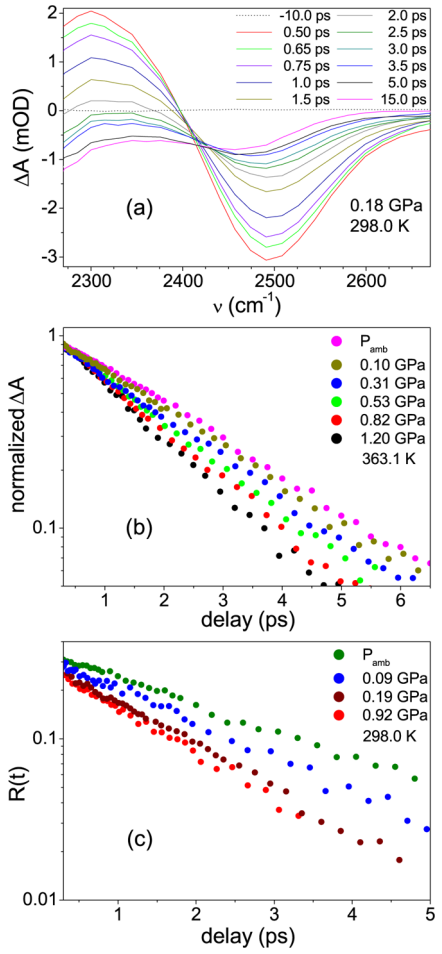

Figure 1. (a) Transient absorption ($\Delta\alpha_{iso}(t)$) spectra of the OD stretching mode measured (0.18 GPa, 298.0 K) at different delays. (b) Semilog plot of temporal evolution of transient absorbance (probe 2580 cm^{-1}) measured at 363.1 K at various pressures. (c) Semilog plot of anisotropy decay $R(t)$ for different pressures at 298.0 K.

Interestingly, at 363 K, τ_R is insensitive to pressure as also very recently observed at 400 K for the rotational diffusion coefficient extracted from quasielastic incoherent neutron scattering (QENS) data.[28] The evolution of the OD lifetime and anisotropy decays with pressure should reflect in the vibrational line width (fwhm). The OD stretching absorption band of HOD was measured along three different isothermal compression paths (273.7, 363.1, and 298.0 K). The absorption band profile was fitted by a single Gaussian function after a linear baseline subtraction. The density evolution of the fwhm, reported in Figure 2, allows the clear identification of two linear regimes with different slopes in the 273.7 and 298.0 K isothermal compressions. With the line broadening determined by the OD lifetime and by the rotational relaxation, we can conclude, looking at the evolution with density of τ_v and τ_R, that the low density broadening is dominated, at 273.7 and 298.0 K, by the orientational term, whereas at high density the vibrational lifetime is the major contribution. At 363.1 K, the fwhm increases linearly with density without slope changes, as the anisotropy and the vibrational lifetime, with a slope characteristic of the high density regime.

A correlation between the structural evolution and the dynamics can be provided by computational methods. We performed classical molecular dynamics simulations at ambient

dx.doi.org/10.1021/jz402302z | J. Phys. Chem. Lett. 2014, 5, 235−240

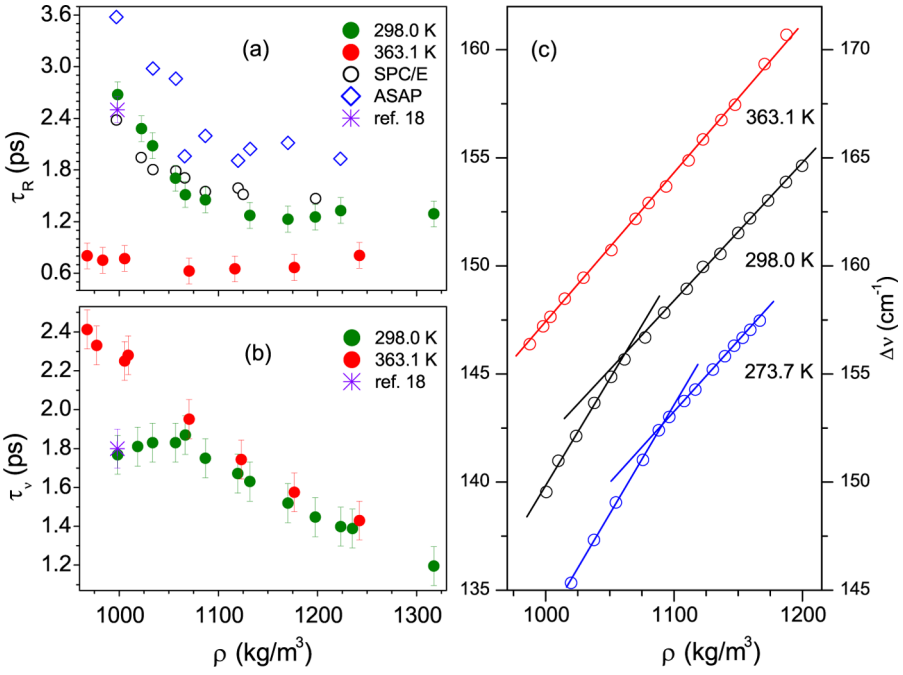

Figure 2. (a) Experimental (full symbols) and ambient temperature computed (open symbols) rotational anisotropy time constant as a function of density at two different temperatures determined by a single exponential fit of $R(t)$. The computed rotational anisotropy decay has been obtained by the time correlation function of the second rank Legendre polynomial of the dipole moment direction unit vector for each HOD molecule.[18] (b) OD stretching lifetime obtained by experimental $\Delta\alpha_{iso}(t)$; (c) fwhm of the OD stretching mode as a function of density. For sake of better comparison the left fwhm scale refers to the 273.7 and 298.0 K traces, and the right scale to the 363.1 K data. Full lines are linear regressions of the experimental data.

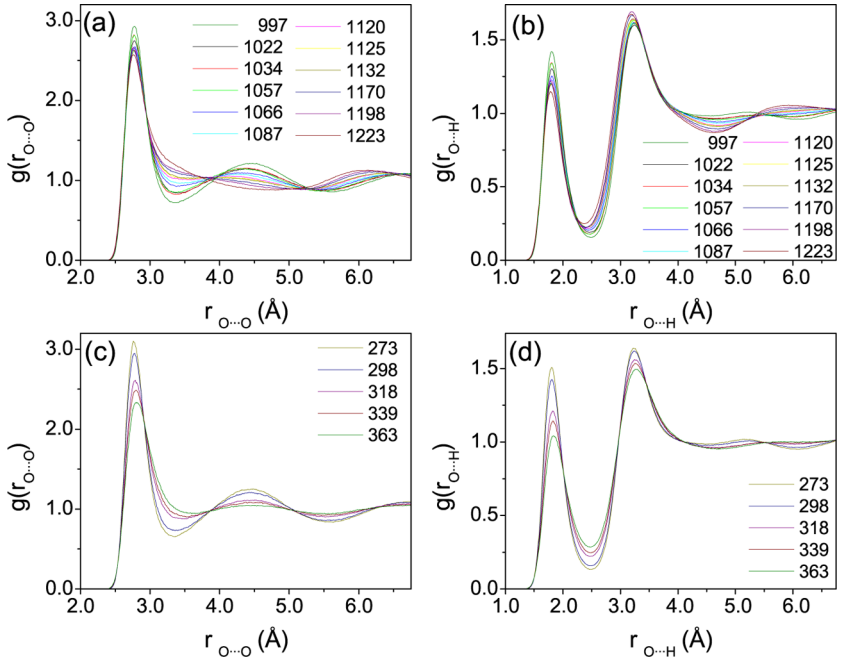

Figure 3. Pair radial distribution function $g(r)$ as obtained by the simulations carried out with the polarizable force field for: (a) O···O at ambient temperature with increasing density (kg/m^3); (b) O···H at ambient temperature with increasing density (kg/m^3); (c) O···O at ambient pressure with increasing temperature (K); and (d) O···H at ambient pressure with increasing temperature (K).

temperature and at densities ranging from 997 (ambient pressure) to 1223 kg/m^3 (0.9 GPa). Standard potentials describing the molecular interactions in water have been tested extensively under ambient conditions, and their transferability to extreme conditions is not guaranteed a priori. Because our study extends to densities 20% higher than ambient, calculations have been performed in the NVE ensemble with the SPC/E model,[29] which was shown to be helpful in the description of ultrafast vibrational spectroscopy experiments,[30] as well as with a recently developed polarizable force field (ASAP) particularly effective in the description of structural properties of water under ambient and extreme conditions.[31]

dx.doi.org/10.1021/jz402302z | J. Phys. Chem. Lett. 2014, 5, 235−240

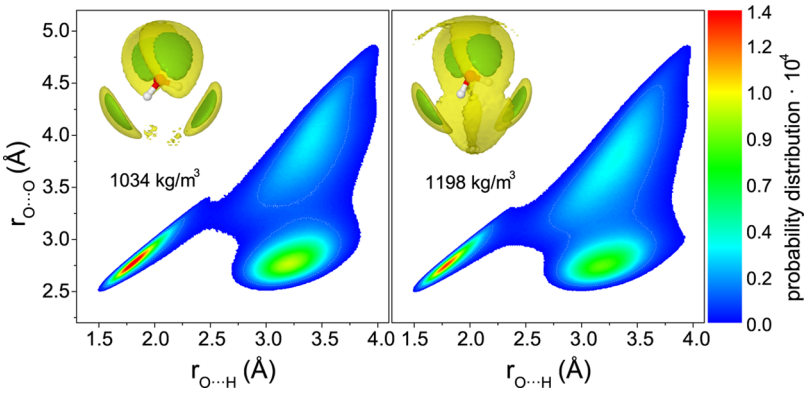

Figure 4. Configurational space at ambient temperature for the water molecules in the first and second solvation shells at two different densities. Insets: space regions representing the probability (isosurfaces cutoff 0.0015) of finding H-bonded (green) and second-shell (yellow) water molecules. The surfaces are smoothed with a Gaussian function for longer distances.

The computed pair radial distribution functions ($g(r)$) (Figure 3) for the O···H contacts show H-bond interactions only slightly perturbed by pressure, in agreement with previous results.[4,5,7] On the contrary, with increasing density the second maximum of the O···O $g(r)$ gradually moves inward and fills the first minimum at ∼3.3 Å. The information obtained from the $g(r)$ at 1034 and 1198 kg/m^3 is summarized in the 2D plots in Figure 4. The surface represents the probability distribution for each O···H and O···O intermolecular distance obtained from the simulation of water at ambient temperature. The two regions ascribable to the first coordination shell are only slightly affected by the density increase, whereas the second shell shifts with increasing density toward the first one occupying the free interstitial sites (Figure 4).

We have also performed classical molecular dynamics simulations at ambient pressure in the 273−363 K temperature range to verify the attainment of the HDW regime with temperature, as suggested by the data reported in Figure 2. From the variations of the O···O pair radial distribution functions (Figure 3), a progressive interpenetration of the first and second shell, caused by an increase in exchange between the molecules of the two shells, is deduced. This behavior is confirmed by the variation in the $g(r)$ for the O···H contacts (Figure 3), which shows a modification of the hydrogen-bond network not observed by increasing the pressure.

The comparison of the spectroscopic data with the computational results highlights how the structural evolution of liquid water with pressure at room temperature corresponds to a dynamical configuration change involving nearest neighbor molecules without altering the local hydrogen-bonded tetrahedral configuration. The connection between experiments and computations is represented by the determination of the rotational anisotropy decay. The values of τ_R computed with the two potentials (Figure 2) share the behavior seen in experiments, namely, an initial decay and a leveling off of the data above ∼1100 kg/m^3. The change in τ_R can be therefore related to the structural changes described previously. The collapse of the second-shell molecules onto the first shell corresponds to an increase in the number of nonbonded molecules at short distances. Consequently, the quantity of equally probable tetrahedral configurations increases, thus facilitating the orientational motion and then shortening the molecular orientational time. These instantaneous events do not appreciably alter the overall number of H bonds and leave the average hydrogen bond connectivity unchanged. This picture is confirmed by the computed mean number of hydrogen bonds formed by the oxygen atom of the water molecules (∼2) that does not change appreciably with increasing pressure. Above ∼1100 kg/m^3, τ_R does not change with further compression, indicating that a limit configuration, in terms of rotational mobility, is achieved. At the same density value, the evolution of the vibrational lifetime also changes abruptly, whereas a clear slope change is observed in the density evolution of the fwhm.

Liquid water can therefore achieve two dynamical regimes, characteristic of LDW and HDW, with different nearest neighbor configurations and ruled by both pressure and temperature. Pressure tunes with continuity the insertion of second-shell molecules in the interstitial sites of the first shell, which results in speeding up the process of breaking and making H bonds without altering the tetrahedral coordination. It is worth remarking that a similar mechanism has been very recently proposed on the basis of the results obtained by a completely different experimental technique (QENS) combined with a molecular dynamics simulation study.[28] Nevertheless, our data, reflecting single-molecule dynamics, allowed us to correlate this continuous structural modification of the liquid driven by pressure to the achievement of the high density configuration. At ambient temperature, this process completes ∼1070 kg/m^3 (0.2 GPa), and no further speeding up of the orientational motion is observed above this value. This structural modification is intimately connected to the change of the dynamical properties revealed by the spectroscopic data. The same properties are also affected by the interpenetration of the first and second shell driven by the temperature: it causes a decrease in the orientational correlation time up to the attainment of a behavior proper of the high-density regime, in which the rotational anisotropy constant is not significantly affected by pressure.

In summary, we find that the modification induced in liquid water by changing pressure and temperature is better described as the crossover between two regimes, for which the usual designation HDW and LDW can be maintained. It is worth noticing that the distinctive character of the two regimes is the dynamic behavior, which results from the interplay of the structural modification induced by pressure and of the temperature effect. A remarkable result is represented by the possibility of revealing the change between the LDW and HDW dynamical regimes by the density dependence of the fwhm of the OD stretching mode, which is an accessible and

dx.doi.org/10.1021/jz402302z | J. Phys. Chem. Lett. 2014, 5, 235−240

reliable experimental method to finely define the $P-T$ region of the two regimes. In Figure 5, the $P-T$ boundary between LDW and HDW regimes is tentatively depicted. It can be seen that a temperature interval of about 10° exists at ambient pressure, just below the boiling point, where water is in the HDW regime.

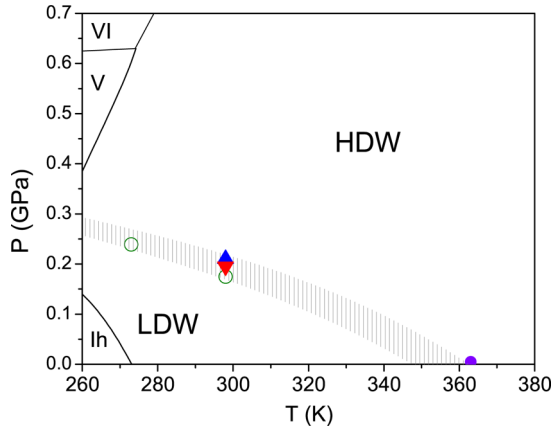

Figure 5. Tentative identification of the P−T regions corresponding to LDW and HDW regimes. Empty dots: slope change of the fwhm versus density; triangles: slope change of experimental (blue) and computed (red) rotational anisotropy with density; full dot: ambient pressure temperature value where water behaves as HDW according to fwhm and rotational anisotropy data. The shaded area is a tentative depiction of the $P-T$ conditions where the limit configuration corresponding to the insertion completion of the second-shell molecules onto the first shell is achieved.

METHODS

A high-pressure membrane cell equipped with high superficial optical quality (5/5 × 0.063 ISO 10110), z-cut, infrared enhanced purity, low-fluorescence sapphire anvils was used. A gilded beryllium-bronze gasket ∼50 μm thick and ∼350 μm in diameter was used to contain the sample. The sample was a 3.5% m/m mixture of D_2O in H_2O (Sigma HPLC grade) mixture corresponding to about 7:100 molar ratio of HOD in H_2O. The fluorescence of a small ruby chip deposited within the sample was used as pressure gauge. The temperature was monitored by use of a calibrated Si-diode fixed in proximity of the sample and a K-type thermocouple soldered to the gasket, with an uncertainty of ±0.1 K.

Infrared measurements were performed with a Bruker-IFS 120 HR FTIR spectrometer modified for high-pressure equipment.[32] High and near-ambient temperatures (363.1 and 298.0 K) were achieved by using a remote-controlled resistive heater, and the low temperature (273.7 K) was achieved by using a closed-cycle helium cryostat. FTIR spectra were recorded with a spectral resolution of 1 cm^{-1} at each temperature as a function of pressure; this was finely tuned by step of ∼0.03 GPa in the whole range of thermodynamic stability of the liquid phase of water.

Mid-IR pump−probe experiments were performed by using the apparatus described in ref 33. In brief, 750 μJ of an amplified Ti-Sapphire laser system (1 kHz, 3 mJ, 35 fs) was used to pump two independent optical parametric amplifiers to generate the pump and the probe and reference pulses. The pump is delayed through a controlled motorized stage and then overlapped to the probe onto the sample. Before the delay stage, the polarization of pump beam was controlled using a waveplate. After the sample, both probe and reference pulses were spectrally dispersed in a spectrometer and imaged separately on a double 32-channel MCT detector providing a spectral resolution of 13 cm^{-1}.

Classical molecular dynamics simulation were performed with the ASAP force field.[31] The starting configurations were obtained by simulation runs carried out with the Moldy program[34] adopting the SPC/E potential,[29] which was shown to be helpful in the description of ultrafast vibrational spectroscopy experiments.[30] Each sample, made up by 96 H_2O and 7 HOD molecules (to reproduce the experimental concentration), was initially thermalized by velocity rescaling at 300 K for 500 ps using the SPC/E potential, followed by an accumulation run of 1 ns with a time step of 0.25 fs, collecting the configurations every 10 steps. Starting from the latest structure, the system was thermalized in the NVT ensemble for ∼50 ps with the polarizable model,[31] integrating the equations of motion with a time step of ∼0.24 fs and collecting the trajectory in the NVE ensemble every 10 steps in the production run of ∼190 ps. The potential parameters adopted during the simulations are reported in ref 31.

AUTHOR INFORMATION

Corresponding Author

*E-mail: roberto.bini@unifi.it.

Notes

The authors declare no competing financial interest.

ACKNOWLEDGMENTS

Supported by European Union (LENS Contract FP7 G.A. no. 284464 LASERLABEUROPE), by Deep Carbon Observatory initiative (grant no. 2011-10-01 from the Alfred P. Sloan Foundation), and by MIUR (grants FIRB - Futuro in Ricerca 2010 RBFR109ZHQ and RBFR10Y5VW and by Regione Toscana through PORFSE 2007-2013 project EPHODS).

REFERENCES

(1) *Water, A Comprehensive Treatise*; Franks, F., Ed.; Plenum Press: New York, 1972−1982.

(2) Mallamace, F. The Liquid Water Polymorphism. *Proc. Natl. Acad. Sci. U.S.A.* **2009**, *106*, 15097−15098.

(3) Laage, D.; Hynes, J. T. A Molecular Jump Mechanism of Water Reorientation. *Science* **2006**, *311*, 832−835.

(4) Soper, A. K.; Ricci, M. A. Structures of High-Density and Low-Density Water. *Phys. Rev. Lett.* **2000**, *84*, 2881−2884.

(5) Strässle, Th.; Saitta, A. M.; Le Godec, Y.; Hamel, G.; Klotz, S.; Loveday, J. S.; Nelmes, R. J. Structure of Dense Liquid Water by Neutron Scattering to 6.5 GPa and 670 K. *Phys. Rev. Lett.* **2006**, *96*, 067801.

(6) Huang, C.; et al. The Inhomogeneous Structure of Water at Ambient Conditions. *Proc. Natl. Acad. Sci. U.S.A.* **2009**, *106*, 15214−15218.

(7) Saitta, A. M.; Datchi, F. Structure and Phase Diagram of High-Density Water: The Role of Interstitial Molecules. *Phys. Rev. E* **2003**, *67*, 020201.

(8) Poole, P. H.; Sciortino, F.; Essmann, U.; Stanley, H. E. Phase Behaviour of Metastable Water. *Nature* **1992**, *360*, 324−328.

(9) Sastry, S.; Debenedetti, P. G.; Sciortino, F.; Stanley, H. E. Singularity-Free Interpretation of the Thermodynamics of Supercooled Water. *Phys. Rev. E* **1996**, *53*, 6144−6154.

(10) Rebelo, L. P. N.; Debenedetti, P. G.; Sastry, S. Singularity-Free Interpretation of the Thermodynamics of Supercooled Water. II. Thermal and Volumetric Behavior. *J. Chem. Phys.* **1998**, *109*, 626−633.

(11) Angell, C. A. Insights Into Phases of Liquid Water From Study of its Unusual Glass-Forming Properties. *Science* **2008**, *319*, 582−587.
(12) Mishima, O.; Stanley, H. E. The Relationship Between Liquid, Supercooled and Glassy Water. *Nature* **1998**, *396*, 329−335.
(13) Nelmes, R. J.; Loveday, J. S.; Strässle, Th.; Bull, C. L.; Guthrie, M.; Hamel, G.; Klotz, S. Annealed High-Density Amorphous Ice Under Pressure. *Nat. Phys.* **2006**, *2*, 414−418.
(14) Krisch, M.; et al. Pressure Evolution of the High-Frequency Sound Velocity in Liquid Water. *Phys. Rev. Lett.* **2002**, *89*, 125502.
(15) Santoro, M.; Gorelli, F. A.; Scopigno, T.; Krisch, M.; Sette, F.; Ruocco, G. Pressure Behavior of the Sound Velocity of Liquid Water at Room Temperature in the Terahertz Regime. *Phys. Rev. B* **2011**, *84*, 092301.
(16) Li, F.; Cui, Q.; He, Z.; Cui, T.; Zhang, J.; Zhou, Q.; Zou, G.; Sasaki, S. High Pressure-Temperature Brillouin Study of Liquid Water: Evidence of the Structural Transition From Low-Density Water to High-Density Water. *J. Chem. Phys.* **2005**, *123*, 174511.
(17) Kawamoto, T.; Ochiai, S.; Kagi, H. Changes in the Structure of Water Deduced From the Pressure Dependence of the Raman OH Frequency. *J. Chem. Phys.* **2004**, *120*, 5867−5870.
(18) Bakker, H. J.; Skinner, J. L. Vibrational Spectroscopy as a Probe of Structure and Dynamics in Liquid Water. *Chem. Rev.* **2010**, *110*, 1498−1517.
(19) Fecko, C. J.; Eaves, J. D.; Loparo, J. J.; Tokmakoff, A.; Geissler, P. L. Ultrafast Hydrogen-Bond Dynamics in the Infrared Spectroscopy of Water. *Science* **2003**, *301*, 1698−1702.
(20) Cowan, M. L.; Bruner, B. D.; Huse, N.; Dwyer, J. R.; Chugh, B.; Nibbering, E. T. J.; Elsaesser, T.; Miller, R. J. D. Ultrafast Memory Loss and Energy Redistribution in the Hydrogen Bond Network of Liquid H_2O. *Nature* **2005**, *434*, 199−202.
(21) Moilanen, D. E.; Fenn, E. E.; Lin, Y. S.; Skinner, J. L.; Bagchi, B.; Fayer, M. D. Water Inertial Reorientation: Hydrogen Bond Strength and the Angular Potential. *Proc. Natl. Acad. Sci. U.S.A.* **2008**, *105*, 5295−5300.
(22) Piatkowski, L.; Eisenthal, K. B.; Bakker, H. J. Ultrafast Intermolecular Energy Transfer in Heavy Water. *Phys. Chem. Chem. Phys.* **2009**, *11*, 9033−9038.
(23) Steinel, T.; Asbury, J. B.; Zheng, J.; Fayer, M. D. Watching Hydrogen Bonds Break: A Transient Absorption Study of Water. *J. Phys. Chem. A* **2004**, *108*, 10957−10964.
(24) Rezus, Y. L. A.; Bakker, H. J. On the Orientational Relaxation of HDO in Liquid Water. *J. Chem. Phys.* **2005**, *123*, 114502.
(25) Rezus, Y. L. A.; Bakker, H. J. Orientational Dynamics of Isotopically Diluted H_2O and D_2O. *J. Chem. Phys.* **2006**, *125*, 144512.
(26) Volkov, V. V.; Palmer, D. J.; Righini, R. Heterogeneity of Water at the Phospholipid Membrane Interface. *J. Phys. Chem. B* **2007**, *111*, 1377−1383.
(27) Wagner, W.; Pruss, A. The IAPWS Formulation 1995 for the Thermodynamic Properties of Ordinary Water Substance for General and Scientific Use. *J. Phys. Chem. Ref. Data* **2002**, *31*, 387−535.
(28) Bove, L. E.; Klotz, S.; Strässle, Th.; Koza, M.; Teixeira, J.; Saitta, A. M. Translational and Rotational diffusion in Water in the Gigapascal Range. *Phys. Rev. Lett.* **2013**, *111*, 185901.
(29) Berendsen, H. J. C.; Grigera, J. R.; Straatsma, T. P. The Missing Term in Effective Pair Potentials. *J. Phys. Chem.* **1987**, *91*, 6269−6271.
(30) Schmidt, J. R.; Roberts, S. T.; Loparo, J. J.; Tokmakoff, A.; Fayer, M. D.; Skinner, J. L. Are Water Simulation Models Consistent with Steady-State and Ultrafast Vibrational Spectroscopy Experiments? *Chem. Phys.* **2007**, *341*, 143−157.
(31) Pinilla, C.; Irani, A. H.; Seriani, N.; Scandolo, S. Ab Initio Parameterization of an All-Atom Polarizable and Dissociable Force Field for Water. *J. Chem. Phys.* **2012**, *136*, 114511.
(32) Bini, R.; Ballerini, R.; Pratesi, G.; Jodl, H. J. Experimental Setup for Fourier Transform Infrared Spectroscopy Studies in Condensed Matter at High Pressure and Low Temperatures. *Rev. Sci. Instrum.* **1997**, *68*, 3154−3160.
(33) Touron Touceda, P.; Vázquez, S. M.; Lima, M.; Lapini, A.; Foggi, P.; Dei, A.; Righini, R. Transient Infrared Spectroscopy: a New Approach to Investigate Valence Tautomerism. *Phys. Chem. Chem. Phys.* **2012**, *14*, 1038−1047.
(34) Refson, K. Moldy: a Portable Molecular Dynamics Simulation Program for Serial and Parallel Computers. *Comput. Phys. Commun.* **2000**, *126*, 310−329.